

---

# In Vivo Measurement of Carbon-11 Thymidine Uptake in Non-Hodgkin's Lymphoma Using Positron Emission Tomography

Ph. Martiat, A. Ferrant, D. Labar, M. Cogneau, A. Bol, C. Michel, J.L. Michaux, and G. Sokal

*Department of Hematology, University of Louvain, Medical School, Brussels; and Positron Emission Tomography Laboratory, University of Louvain, Louvain-la-Neuve, Belgium*

Carbon-11 thymidine (TdR) uptake using positron emission tomography (PET) has been measured in ten patients with non-Hodgkin's lymphoma (NHL). The rate of TdR uptake (mean  $\pm$  s.d.) was of  $0.009 \pm 0.006 \mu\text{mol} \cdot 100 \text{ cc}^{-1} \cdot \text{min}^{-1}$  in low-grade NHL. This rate was  $0.063 \pm 0.049 \mu\text{mol} \cdot 100 \text{ cc}^{-1} \cdot \text{min}^{-1}$  in intermediate-grade NHL and  $0.159 \mu\text{mol} \cdot 100 \text{ cc}^{-1} \cdot \text{min}^{-1}$  in a patient with high-grade NHL. Lymphoma radioactivity reached a plateau at  $0.42 \pm 0.22 \%$   $100 \text{ cc}^{-1}$  of the injected dose from 10 min after injection. The highest  $^{11}\text{C}$  uptakes were observed in the kidneys and in the liver ( $3.30 \pm 1.30$  and  $2.10 \pm 0.05 \%$   $100 \text{ cc}^{-1}$  of the injected dose, respectively). The lymphoma-to-muscle ratio was of  $11.8 \pm 1.7$ , whereas the lymphoma-to-intestine ratio was of  $1.5 \pm 0.7$ . Accordingly, the measurement of [ $^{11}\text{C}$ ]TdR uptake in the abdomen may need other imaging methods for adequate interpretation. The results suggest that [ $^{11}\text{C}$ ]TdR uptake using PET might be a method for noninvasively measuring cell proliferation in vivo.

J Nucl Med 29: 1633-1637, 1988

---

**T**hymidine (TdR) is used in DNA synthesis and is taken up by dividing cells. Most often, the rate of uptake of TdR can be regarded as an index of cell proliferation (1,2). Positron emission tomography (PET) and carbon-11 ( $^{11}\text{C}$ ) TdR (3) would give the opportunity to measure the rate of uptake of TdR noninvasively in vivo.

Cell proliferation is an important prognostic factor in malignant disease (4-6) and may have therapeutic implications (7). In non-Hodgkin's lymphoma (NHL) particularly, treatment can depend on the grade of malignancy and this grade is most often assessed by means of histopathology. Morphology, however, does not always give adequate information on the rate of cell proliferation. Carbon-11 ( $^{11}\text{C}$ ) TdR uptake using PET has been investigated in NHL patients to evaluate its feasibility and to obtain an index of cell proliferation.

## PATIENTS AND METHODS

### Patients

Ten patients with NHL were studied (Table 1). Lymph node histology was classified according to the Working Formulation (8). One patient had high-grade lymphoma, five intermediate-grade, and four low-grade lymphoma. Seven patients were evaluated at admission and three at relapse. The relapsed patients were off therapy at the time of the investigation.

### Methods

Carbon-11 methyl TdR was synthesized using a procedure (9) adapted from that described by Sundoro-Wu et al. (10). Carbon-11 methyl iodide was prepared by the reaction between [ $^{11}\text{C}$ ]methanol and diphosphorous tetraiodide at  $85^\circ\text{C}$ . It was purified at  $55^\circ\text{C}$  through a column packed with soda lime and  $\text{P}_2\text{O}_5$  and then trapped in 1 ml of tetrahydrofuran (THF) at  $-78^\circ\text{C}$ . The addition of 1  $\mu\text{mol}$  methyl iodide was followed by that of 2 mg sodium hydride.

The TdR precursor was prepared in THF at  $-78^\circ\text{C}$  by the reaction of Eq. (2) 1.6 N n-butyllithium with the tetrahydropyranyl derivative of 5-bromodeoxyuridine (0.04 mmol). This

---

Received Nov. 9, 1987; revision accepted Apr. 19, 1988.

For reprints contact: A. Ferrant, MD, Cliniques Universitaires St-Luc, 10, Avenue Hippocrate, B-1200 Brussels, Belgium.

**TABLE 1**  
Patient Characteristics

Patient no.	Age/sex	Site of measurement	Histologic subtype
1	72/M	Axilla	Small lymphocytic (SL)
2	64/F	Axilla	Small lymphocytic (SL)
3	65/M	Axilla	Small lymphocytic (SL)
4	47/F	Abdomen	Follicular, predominantly small cleaved cell (FSC)
5	60/M	Mediastinum	Follicular, predominantly large cell (FLC)
6	65/M	Epigastrium	Follicular, predominantly large cell (FLC)
7	37/M	Mediastinum	Diffuse, mixed small and large cell (DM)
8	47/M	Epigastrium	Diffuse, mixed small and large cell (DM)
9	47/M	Abdomen	Diffuse, mixed small and large cell (DM)
10	38/M	Abdomen	Lymphoblastic (LBL)

precursor solution was added to the [<sup>11</sup>C]methyl iodide solution at -23°C. After stirring for 6 min, the reaction was quenched with 1N HCl in methanol (0.8 ml). Tetrahydropyran-yl protecting groups were removed by heating at 60°C for 5 min. After cooling, the crude mixture was neutralized to pH 7. Solvents were eliminated under vacuum. Carbon-11 TdR was isolated using semi-preparative high performance liquid chromatography (HPLC) (Serva octadecyl 10 μ; water-methanol, 9:1; retention time 4 min). Starting from [<sup>11</sup>C] carbon dioxide, the decay-corrected radiochemical yield was 50%. Specific activity ranged from 370 to 550 GBq/mmol. Total synthesis time was 45 min.

Toxicity studies and screening for pyrogens were performed in rats, rabbits, and monkeys. PET scans were obtained using an ECAT III one-ring scanner, the characteristics and performances of which have been described previously (11). With the chosen collimator aperture, the effective slice thickness was 15 mm (FWHM). To correct for attenuation, a transmission scan was obtained using an external germanium-68 ring source. To avoid the partial volume effect, measurements were performed on tumor masses larger than 4 cm.

The plasma TdR concentration at the time of the study was measured using HPLC as described by Bodycote and Wolff (12). A catheter was placed in the radial or femoral artery. Carbon-11 TdR (250-500 MBq) was injected intravenously over 3 min. Arterial blood samples were obtained at 30-sec intervals during the first 5 min, at 1-min intervals during next 10 min, and later at 5-min intervals to obtain the input curve. From 10 min after the start of the study, labeled metabolites of TdR interfered with plasma [<sup>11</sup>C]TdR. These metabolites were eliminated as follows. After deproteinization, the plasma was filtered on an ion exchange resin (Deaminac

F-4 filter R) to remove beta-ureidoisobutyrate and beta-aminoisobutyrate. Labeled carbon dioxide disappeared from the blood samples during the procedure.

Scans were performed in a dynamic mode at 0, 1, 2, 3, 4, 6, 8, 10, 13, 16, 19, 24, 29, 34, and 40 min. 1-1.5 × 10<sup>6</sup> total coincidence counts were collected in each scan. Beyond 40 min the count rate was too low to acquire data with sufficient statistical precision.

For mediastinal and abdominal lymphomas, a CT scan was used to position the patient in the PET scanner.

The study has been approved by the local ethics committee.

#### Description of the Theoretical Model

The metabolism of TdR can be outlined using a three-compartment model (Fig. 1).

The three compartments include the plasma TdR (P), the intracellular TdR (I) and phosphorylated TdR (L). There are three rate constants: the rate of disappearance of TdR from plasma to cytoplasm (k<sub>1</sub>), the rate of TdR degradation (k<sub>2</sub>) and the rate of TdR phosphorylation (k<sub>3</sub>). The model assumes that most of the TdR that has been taken up in the cell is either used for DNA synthesis or is degraded. The labeled metabolites should not be reutilized for DNA synthesis and [<sup>11</sup>C]TdR should not be degraded in the plasma during the experiment. Other assumptions are that exogenous and endogenous thymidine behave similarly and that the tracer is homogeneously distributed in the area of interest. Furthermore, a steady state is assumed.

The tomographic area of interest includes events related to both I\* and L\*. The corresponding differential equations are:

$$dI^*/dt = k_1^* \cdot P^* - k_2^* \cdot I^* - k_3^* \cdot I^* \quad (1)$$

$$dL^*/dt = k_3^* \cdot I^* \quad (2)$$

The activity recorded by the scanner is:

$$(I^* + L^* = k_1^*/(k_2^* + k_3^*))$$

$$\cdot [k_3^* + k_2^* \cdot e^{-(k_2^* + k_3^*)t}] \times P^* \quad (3)$$

where X is the convolution product, and P\* the metabolite-free plasma activity.

To obtain the rate constants k<sub>1</sub><sup>\*</sup>, k<sub>2</sub><sup>\*</sup> and k<sub>3</sub><sup>\*</sup> the time-activity curve of the region of interest was corrected for decay and attenuation and fitted to Eq. (3) using a nonlinear least square fit program (13).

As the plasma TdR concentration (P) is known, the phosphorylation rate of TdR in the area of interest can be calcu-

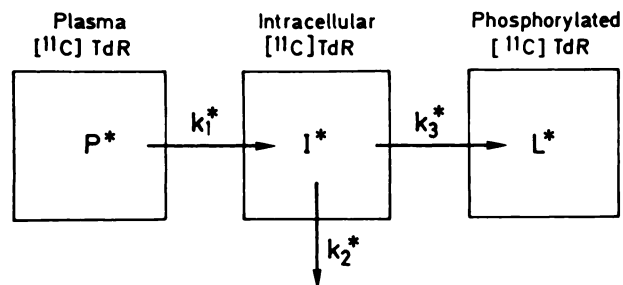


**FIGURE 1**  
Model for the kinetic evaluation of [<sup>11</sup>C]TdR.

**TABLE 2**  
Uptake of [<sup>11</sup>C]Thymidine by Lymphoma

Patient no. (histologic subtype)	% Dose · 100 cc <sup>-1</sup>	Plasma TdR (μmol · l <sup>-1</sup> )	Rate of uptake (μmol · 100 cc <sup>-1</sup> · min <sup>-1</sup> )
1 (SL)	0.15	2.6	0.005
2 (SL)	0.47	4.0	0.019
3 (SL)	0.27	1.5	0.005
4 (FSC)	0.25	2.2	0.008
5 (FLC)	0.76	15.0	0.015
6 (FLC)	0.50	6.8	0.018
7 (DM)	0.71	8.6	0.134
8 (DM)	0.95	8.5	0.079
9 (DM)	0.63	8.4	0.070
10 (LBL)	1.03	17.5	0.159

lated and expressed as μmol · 100 cc<sup>-1</sup> · min<sup>-1</sup>

$$dL/dt = \frac{k_1 \cdot k_3}{k_2 + k_3} \cdot P$$

where the rate constants k<sub>1</sub>, k<sub>2</sub>, and k<sub>3</sub> are identical to the ones obtained using [<sup>11</sup>C]TdR.

## RESULTS

The time-activity curves of the lymphomatous masses after injection of [<sup>11</sup>C]TdR were characterized by a rapid rise in activity with a maximum uptake of 0.54 ± 0.19% · 100 cc<sup>-1</sup> of injected activity at 5 min. Thereafter, activity decreased, and a plateau was observed from 10 min on. At 30 min, the uptake in lymphoma was 0.42 ± 0.22% · 100 cc<sup>-1</sup>, range 0.15 – 1.03 (Fig. 2, Table 2).

The concentration of the tracer was highest in the kidneys and in the liver. At 30 min, the uptake was 3.40 ± 1.17% · 100 cc<sup>-1</sup> and 2.40 ± 0.28% · 100 cc<sup>-1</sup> in the kidneys and liver, respectively. In both these organs

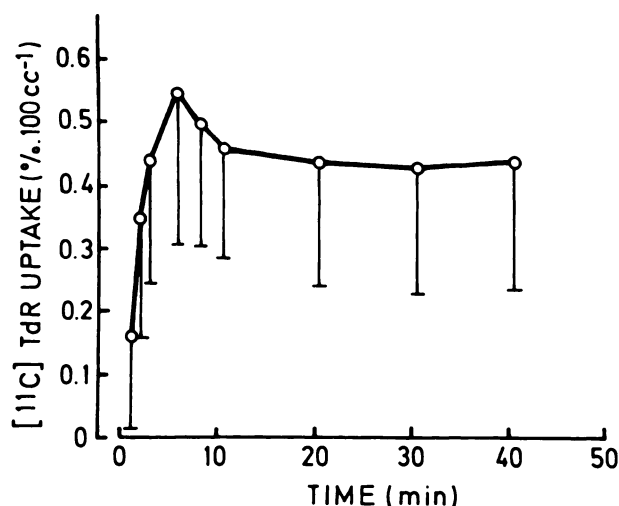


**FIGURE 2**  
Time course of [<sup>11</sup>C]TdR uptake in lymphoma (mean – s.d.). All the patients are included and the data are corrected for decay.

an uptake plateau was observed from 10 min after starting the injection.

The uptake in the spleen and in the intestine was within the range of uptake in lymphoma, whereas the uptake was low in lung and in muscle (Table 3).

Accordingly, the lymphoma-to-muscle ratio and lymphoma-to-lung ratio were high (11.8 ± 1.7 and 4.6 ± 0.3, respectively, Table 4), whereas the lymphoma-to-liver and lymphoma-to-kidney ratios were low. The lymphoma-to-intestine ratio was 1.55 ± 0.68. So lymphomas were easily visualized in the mediastinum, the axillary or cervical regions, but not always in the abdominal region because of the high surrounding activity.

Uptake in low-grade lymphoma was low, at 0.28 ± 0.13% · 100 cc<sup>-1</sup>, whereas uptake in the patient with high-grade lymphoma was markedly higher (1.03% · 100 cc<sup>-1</sup>). In intermediate-grade lymphoma, uptake was in between, at 0.72 ± 0.16% · 100 cc<sup>-1</sup>. So, in this limited series of patients, the fractional uptake of [<sup>11</sup>C]TdR in lymphoma corresponded to the histologic grade of malignancy.

The rates of uptake in TdR in lymphomatous tissue (Fig. 3) varied more widely than the fractional uptake. The fractional uptake of [<sup>11</sup>C]TdR varied over a seven-fold range, and the rates of uptake over a 32-fold range (Table 2). Here again, low-grade and high-grade lymphoma had the lowest and highest rates of uptake, respectively, with 0.009 ± 0.006 μmol · 100 cc<sup>-1</sup> · min<sup>-1</sup> in low-grade lymphoma and 0.159 μmol · 100 cc<sup>-1</sup> · min<sup>-1</sup> in high-grade lymphoma. The rates of uptake in intermediate-grade lymphoma varied widely, from 0.015 μmol · 100 cc<sup>-1</sup> · min<sup>-1</sup> to 0.070 μmol · 100 cc<sup>-1</sup> · min<sup>-1</sup>. The mean uptake in this patient group was 0.063 ± 0.049 μmol · 100 cc<sup>-1</sup> · min<sup>-1</sup>. In two patients with intermediate-grade lymphoma the rate of uptake was similar to that observed in low-grade lymphoma.

For the rate of uptake of TdR, the accuracy of the measurements was within ±25%.

## DISCUSSION

This study suggests that PET-scanning using [<sup>11</sup>C] TdR would provide a noninvasive tool for assessing the proliferation of tumors in vivo. The method we used for the measurement of the rate of TdR uptake needs comment. Because of the short physical half-life of the tracer, the data are derived from events recorded until 40 min after injection of [<sup>11</sup>C]TdR. At that time, most of the injected TdR that is not metabolized is phosphorylated and bound to be utilized for DNA synthesis (14).

The rate of uptake of exogenous TdR into cell DNA may depend on many factors: the blood supply, the relative contribution of endogenous synthesis of TdR, the extra- and intracellular concentration of TdR, its

**TABLE 3**  
Uptake of [<sup>11</sup>C]Thymidine by Organs\*

Organ (patients studied)	Time after injection (min)				
	5	10	20	30	40
Lung (4)	0.43 (0.15)	0.31 (0.16)	0.23 (0.11)	0.16 (0.12)	0.15 (0.12)
Kidney (4)	2.95 (1.07)	3.10 (1.58)	3.30 (1.43)	3.40 (1.17)	3.30 (1.30)
Liver (3)	1.85 (0.78)	2.35 (0.49)	2.55 (0.49)	2.40 (0.28)	2.10 (0.57)
Spleen (3)	1.14 (0.33)	1.05 (0.27)	0.98 (0.29)	0.95 (0.30)	0.91 (0.28)
Intestine (4)	0.61 (0.15)	0.53 (0.15)	0.49 (0.16)	0.45 (0.15)	0.44 (0.17)

\* % dose · 100 cc<sup>-1</sup>, mean (s.d.).

cellular uptake and metabolism and, finally, the activity of TdR kinase. Recently, it has been shown that TdR uptake in tumor is independent of blood flow (15) and that endogenous and exogenous thymidine behave similarly (16). In our model, the plasma TdR concentration is known, but we have no assessment of intracellular TdR. This unknown factor might affect the accuracy of the data.

Metabolites of [<sup>11</sup>C]TdR could also interfere. Since TdR disappears very rapidly from the plasma after intravenous injection (17) its degradation in the plasma is not important (12). TdR disappearance from plasma should take place largely by cellular uptake. Intracellular degradation of TdR rapidly results in thymine, beta-ureidoisobutyrate, beta-aminoisobutyrate, carbon dioxide and water, with no metabolite left in the blood by 1 hr after injection (14). Degradation of TdR once phosphorylation has started should be minor in comparison with the intracellular degradation. No reutilization of <sup>11</sup>C occurs during the study (16), and the plasma curve has been corrected for circulating metabolites. Thus, errors due to the activity from metabolites are unlikely to be important.

The extracellular concentration in TdR affects the fractional uptake of labeled TdR (14), and accordingly the rate of uptake could be a better index of cell proliferation.

Although the three-compartment model we used for

**Table 4**  
Lymphoma-to-Tissue Ratios at 30 min

Lymphoma-to-liver	0.26 (0.18–0.32)
Lymphoma-to-kidney	0.18 (0.16–0.25)
Lymphoma-to-lung	4.60 (4.40–4.80)
Lymphoma-to-intestine	1.55 (1.10–2.50)
Lymphoma-to-muscle	12.00 (10.10–14.30)

\* Mean (range).

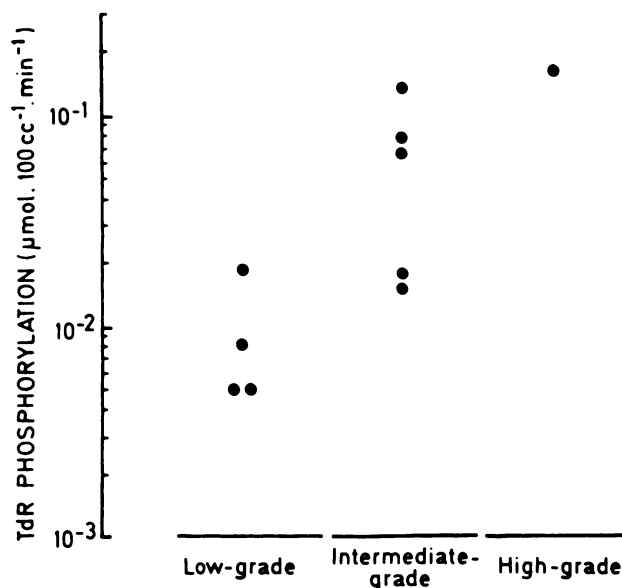


**FIGURE 3**  
Rate of uptake of TdR in lymphoma according to histologic subtype.

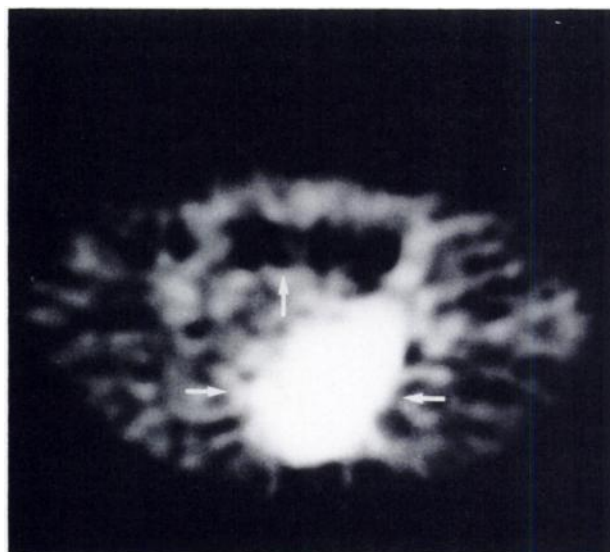


**FIGURE 4**  
Carbon-11 TdR PET scan of the lower pelvis, with uptake in a lymphomatous mass (two arrows). The area without activity corresponds to the urinary bladder (one arrow).

measurement of thymidine uptake is presumably a simplification, we believe that the data are likely to reflect the reality. It must be noted that the in vivo uptake of TdR in a tumor may not only concern malignant cells but possibly also normal cells.

After intravenous injection, [<sup>11</sup>C]TdR distribution was characterized by high kidney and liver uptake. Assuming a weight of 1,500 g for the liver and 300 g for both kidneys, this means that the uptakes of [<sup>11</sup>C]TdR by these organs are of 35% and 10% of the injected dose, respectively. The fractional uptake and the concentration of [<sup>11</sup>C]TdR in liver and kidneys are largely superior to those observed in lymphoma. Uptake in the intestine was also substantial, and lymphoma-to-intestine ratios were in the range where other imaging methods were needed to guide PET.

In vitro uptake of TdR\* by lymphoma cells has prognostic significance (1,5). Theoretically, the "in vivo" measurement of TdR\* uptake should provide better information. The present data suggest that the measurement of "in vivo" uptake of TdR\* reflects the findings of histopathology in the patients with low-grade lymphoma and high-grade lymphoma. It is of interest that the range of the rates of uptake in intermediate grade lymphoma was extremely large, and this illustrates the heterogeneity of this group of lymphomas.

Carbon-11 TdR and PET might be especially of use for the evaluation of proliferative activity of lymphoma in the mediastinum or in the abdomen where direct access often needs surgery. Another advantage is the possibility of repeated studies. Further experience is warranted and needed to better define the potential and the indications of the method.

#### ACKNOWLEDGMENTS

This work has been supported by Grant No. 3.4548.87, FRSM. M.P. Berckmans skillfully typed the manuscript.

#### REFERENCES

1. Hughes WL, Bond VP, Brecher, G, et al. Cellular proliferation in the mouse revealed by autoradiography with tritiated thymidine. *Proc Natl Acad Sci USA* 1958; 44:476-483.
2. Lea MA, Morris HP, Weber G. Comparative biochemistry of hepatomas. VI. Thymidine incorporation into DNA as a measure of hepatoma growth rate. *Cancer Res* 1966; 26:465-469.
3. Christman D, Crawford EJ, Friedkin M, et al. Detection of DNA synthesis in intact organisms with positron-emitting methyl-[<sup>11</sup>C] thymidine. *Proc Natl Acad Sci USA* 1972; 69:988-992.
4. Meyer JS, Friedman E, McCrate MM, et al. Prediction of early course of breast carcinoma by thymidine labeling. *Cancer* 1983; 51:1879-1886.
5. Costa A, Bonadonna G, Villa E, et al. Labeling index as a prognostic marker in non-Hodgkin's lymphomas. *JNCI* 1981; 66:1-5.
6. Hansen H, Koziner B, Clarkson B. Marker and kinetic studies in the non-Hodgkin's lymphomas. *Am J Med* 1981; 71:107-123.
7. Shackney SE, McCormack GW, Cuchural GJ. Growth rate patterns of solid tumors and their relation to responsiveness to therapy. An analytic review. *Ann Int Med* 1978; 89:107-121.
8. The non-Hodgkin's lymphoma pathologic classification project. National Cancer Institute sponsored study of classifications of non-Hodgkin's lymphomas. Summary and description of a Working Formulation for clinical usage. *Cancer* 1982; 49:2112-2135.
9. Labar D, Cogneau M. Radiochemical preparation of [<sup>11</sup>C] thymidine for positron tomography [Abstract]. *Nucl Med* 1987; 26:196.
10. Sundoro-Wu BM, Schmall B, Conti PS, et al. Selective alkylation of pyrimidyl-dianions: synthesis and purification of [<sup>11</sup>C] labeled thymidine for tumor visualization using positron emitting tomography. *Int J Appl Radiat Isot* 1984; 35:705-708.
11. Hoffman EJ, Phelps ME, Huang SC, et al. Dynamic, gated and high resolution imaging with the ECAT III. *IEEE Trans Nucl Sci* 1986; 33:452-455.
12. Bodycote J, Wolff S. Metabolic breakdown of 3H thymidine and the inability to measure human lymphocyte proliferation by incorporation of radioactivity. *Proc Natl Acad Sci USA* 1986; 83:4749-4753.
13. James F, Roos M. MINUIT package. CERN computer center, program library, 1985.
14. Cleaver JE. Thymidine metabolism and cell kinetics. *Frontiers Biol* 1967; 6:43-91.
15. Shields AF, Larson SM, Grunbaum Z, et al. Short-term thymidine uptake in normal and neoplastic tissues: studies for PET. *J Nucl Med* 1984; 25:759-764.
16. Shields AF, Quackenbush RC, Coonrod DV, et al. Development of C-11 thymidine as a PET imaging agent: biochemistry of its synthesis, degradation, and reutilization [Abstract]. *J Nucl Med* 1986; 27:1033.
17. Rubini RR, Cronkite EP, Bond VP, et al. The metabolism and fate of tritiated thymidine in man. *J Clin Invest* 1960; 39:909-918.